Unexpected Epitaxial Growth of a Few WS_2 Layers on $\{1\bar{1}00\}$ Facets of ZnO Nanowires

Boris Polyakov,*,[a] Krisjanis Smits,[a] Alexei Kuzmin,*,[a] Janis Zideluns,[a] Edgars Butanovs,[a] Jelena Butikova,[a] Sergei Vlassov,[b] Sergei Piskunov,[a] and Yuri F Zhukovskii[a]

[a] *Institute of Solid State Physics, University of Latvia, Kengaraga str. 8, LV-1063 Riga, Latvia.*

[b] *Institute of Physics, University of Tartu, Ravila 14c, 50412 Tartu, Estonia*

Corresponding authors.

*E-mail: boris.polyakov@cfi.lu.lv. Phone: +371-67187511. Fax: +371-67132778.

*E-mail: a.kuzmin@cfi.lu.lv. Phone: +371-67251691. Fax: +371-67132778.

TEM Images of ZnO/WO_3 Core-Shell Nanowire. ZnO nanowires (NWs) were initially coated by a nanothin layer of amorphous a-WO_3 using reactive dc magnetron sputtering of metallic tungsten target in mixed Ar/O_2 atmosphere. The thickness of a-WO_3 layers shown in Figure S1 is about 30 nm in (a) and 10 nm in (b). Then ZnO/a-WO_3 NW samples were annealed in a quartz tube in a sulphur atmosphere during 0.5 h at 800 °C to convert amorphous tungsten trioxide into tungsten disulphide, followed by heating for 0.5 h in inert atmosphere to sublimate some remaining amount of WO_3. The growth of WS_2 sub-layer takes place at the interface between ZnO core and WO_3 shell (c, d).

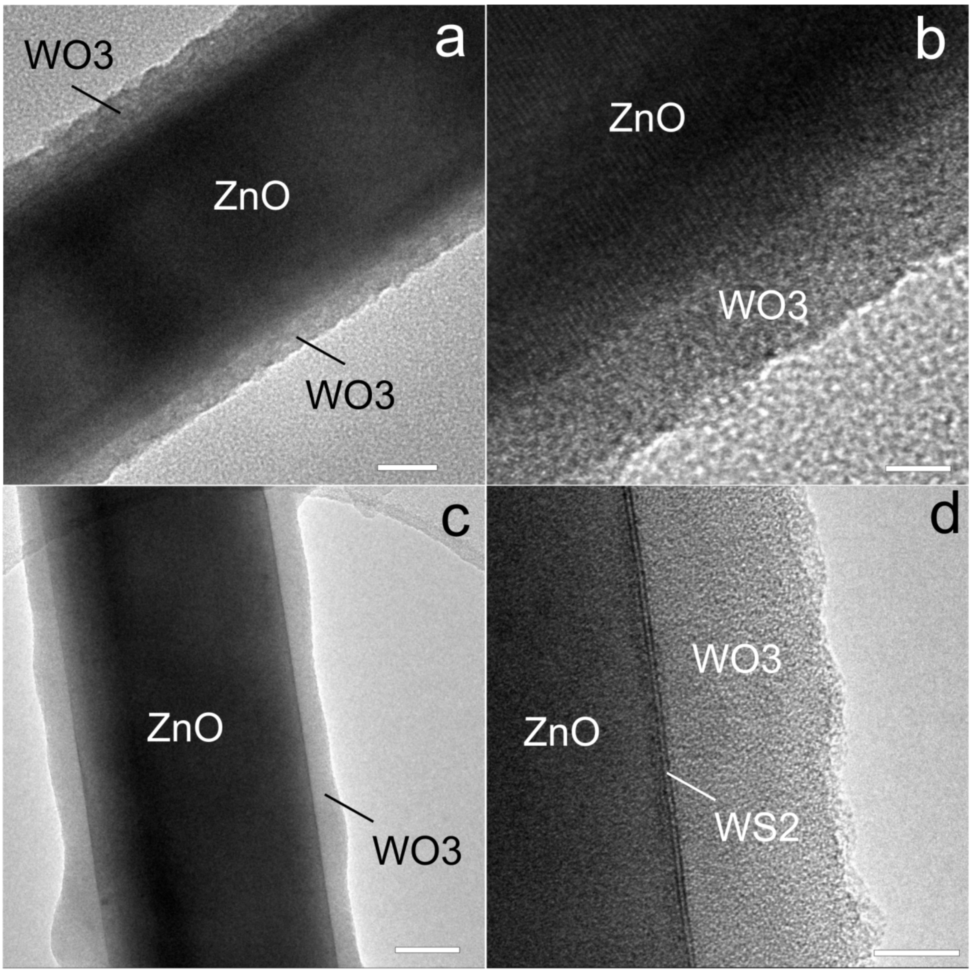

Figure S1. TEM images of ZnO/WO_3 nanowire (a, b), and $ZnO/WS_2/WO_3$ nanowire (c, d) after sulfidation at 800 °C but before annealing in inert atmosphere. Scale bars are 20nm (a), 5 nm (b), 50 nm (c), and 10 nm (d).

Atomistic Prototypes of ZnO($1\bar{1}00$) Substrates with Various Morphologies. The key role in the epitaxial WS_2 film adhesion to [0001]-oriented ZnO nanowire (NW) is played by a family of $\{1\bar{1}00\}$ plane facets not by tiny areas around NW ribs (Figure 1). This is why two-dimensional (2D) model of ZnO($1\bar{1}00$)/WS_2 core-shell interface has been selected for comparison with the experimental data for ZnO$\{1\bar{1}00\}$/WS_2 core-shell NW, while analogous 1D model cannot be applied for large-scale simulation of the interface at all, due to a complexity of its morphology and low NW symmetry compared to the interface slab model.

We have considered two morphologies of defect-less ZnO($1\bar{1}00$) substrate (Table S1): more smooth *n*-type (Figure S2), which is likely exposed in all six facets of [0001]-oriented ZnO NW and more loosened *p*-type (Figure S3). Obviously, the former is energetically more favorable as being observed earlier too (for example, Meyer, B.; Marx, D. *Phys. Rev. B* **2003**, *67*, 035403). On the other hand, the latter is found to be chemically more reactive (Table S2) as is usually found for less smooth and defective surfaces (for example, Wen, C. Z.; Jiang, H. B.; Qiao, S. Z.; Yang, H. G.; Lu, G. Q. *Chem. Commun.* **2011**, *21*, 7052-7061).

Table S1. Energy and geometry parameters of optimized ZnO($1\bar{1}00$) surfaces.

models	interlayer and inter-planar distances			surface energy, E_{surf},* J/m^2	band gap, $\Delta\varepsilon_g$, eV
	$h_{inter\text{-}layer}$	$h_{inter\text{-}plane}$ (n)	$h_{inter\text{-}plane}$ (p)		
S-doped *n*-type	2.60	0.57	2.02	_**	1.39
n-type	2.56	0.54	2.02	1.28	3.36
p-type	2.61	1.09	1.52	3.35	2.12

* $E_{surf} = \dfrac{E_{slab\_\mathrm{UC}} - N_{\mathrm{FU}} E_{bulk\_\mathrm{UC}}}{2S_{slab\_\mathrm{UC}}}$, where E_{slab_UC} and E_{bulk_UC} are the total energies *per* slab unit and bulk formula unit, respectively, *N* is the number of FU *per* slab UC, while S_{slab_UC} is the surface area *per* UC;

** for doped slabs, definition of surface energies has not been properly provided so far.

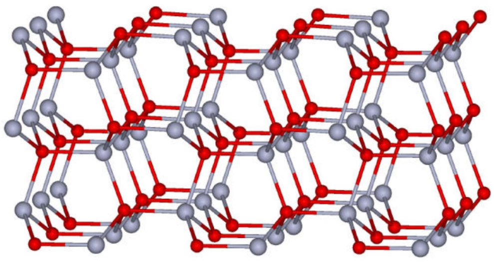

Figure S2. Aside view of 3×3 supercell for *n*-type configuration of ZnO($1\bar{1}00$) substrate. Zn and O atoms are shown by grey-blue and red balls, respectively.

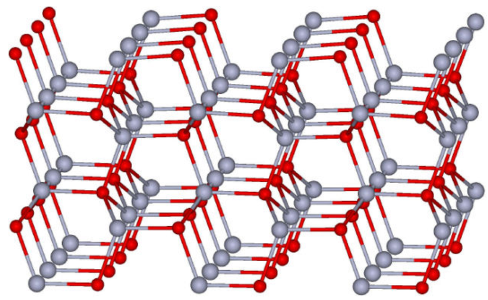

Figure S3. Aside view of 3×3 supercell for *p*-type configuration of ZnO($1\bar{1}00$) substrate. Zn and O atoms are shown by grey-blue and red balls, respectively.

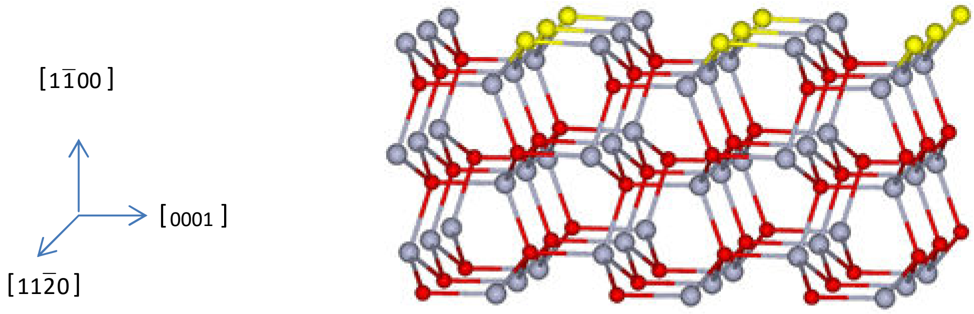

Figure S4. Aside view of 3×3 supercell for *n*-type configuration of S-doped ZnO($1\bar{1}00$) substrate. Zn, O and S atoms are shown by grey-blue, red and yellow balls, respectively.

In the case of S-doped ZnO($1\bar{1}00$) substrate (Figure S4) the value of E_{bind} defined by Equation (1) is smaller than in the case of pure surface (1.59 eV *vs.* 2.10 eV) due to a noticeably larger interfacial distance in the former case (2.03 Å *vs*. 2.16 Å, caused by a larger diameter of S atoms as compared to that for O). It is also clear from Table S2 that the outer layer of pristine *p*-type ZnO substrate is noticeably relaxed as compared to internal layers of its slab model.

Selected Area Electron Diffraction (SAED) of ZnO/WS_2 Core-Shell Nanowire. The SAED pattern of ZnO/WS_2 NW is shown in Figure S5(a) along with its TEM image (b). The clear diffraction spots indicate the high crystallinity of the system. The diffraction pattern was processed by CrysTBox software (Klinger, M.; Jäger, A. *J. Appl. Crystallogr*. **2015**, *48*, 2012-2018). The SAED pattern from the NW core is identified in (d,f) as a hexagonal ZnO-zincite structure with the $\langle 11\overline{2}0\rangle$ zone axis, whereas the SAED pattern from WS_2 layers is identified as tungstenite (Crystallography Open Database (COD) card number 9012191) with the $\langle 1\overline{2}13\rangle$ zone axis.

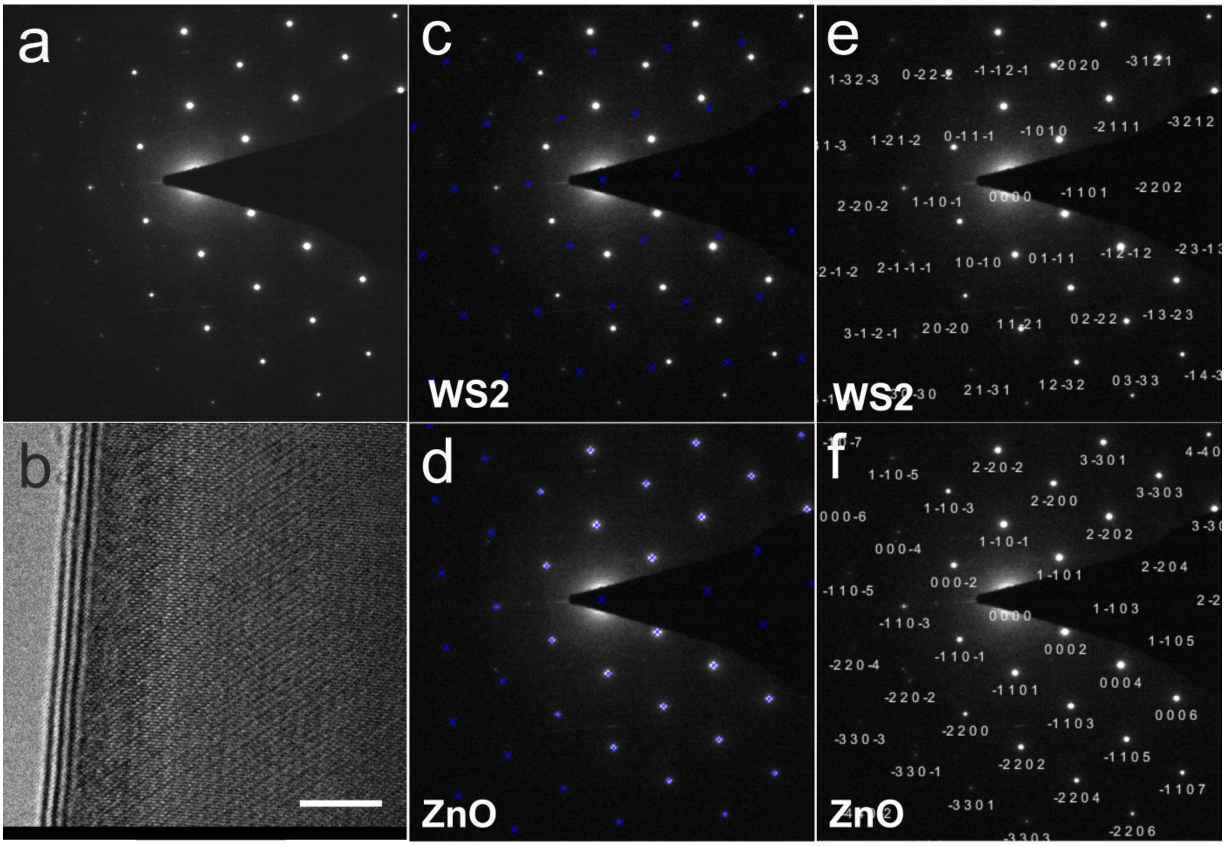

Figure S5. The SAED pattern (a) of ZnO/WS_2 core-shell NW (b) and its analysis (c-f). Scale bar is 5 nm in (b).

Atomistic Models of sWS_2/S-covered ZnO($1\bar{1}00$) Core-Shell Interfaces. In our simulations on submonolayer-structured WS_2 bridging groups upon the S-doped ZnO($1\bar{1}00$) substrate, we have considered three configurations shown in Figures 6(d-f): 0.5ML, both striped (Figure S6) and net (Figure S7), as well as net 0.25ML (Figure S8).

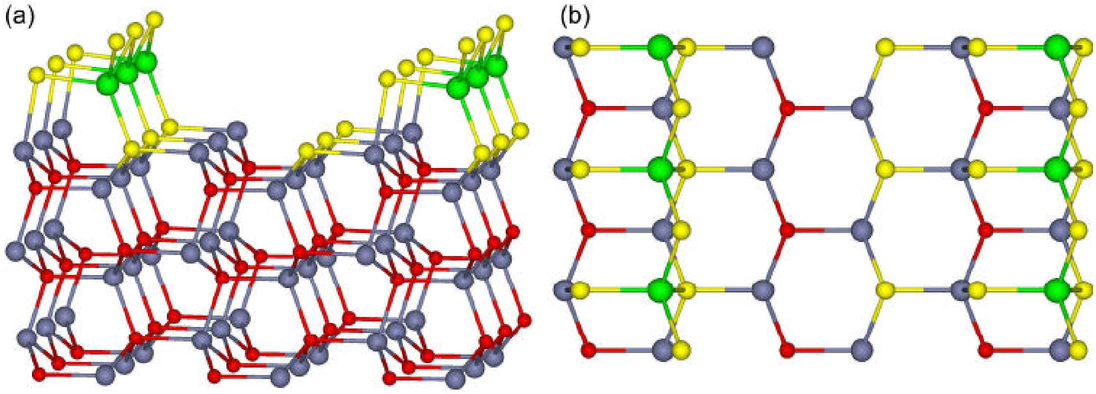

Figure S6. Aside (a) and atop (b) views of 3×3 supercells for S-doped ZnO($1\bar{1}00$)/*s*WS_2 interface with *n*-type morphology of substrate and 0.5ML striped configuration of adsorbate. Small red, middle yellow, middle grey-blue and large green balls correspond to O, S. Zn and W atoms, respectively.

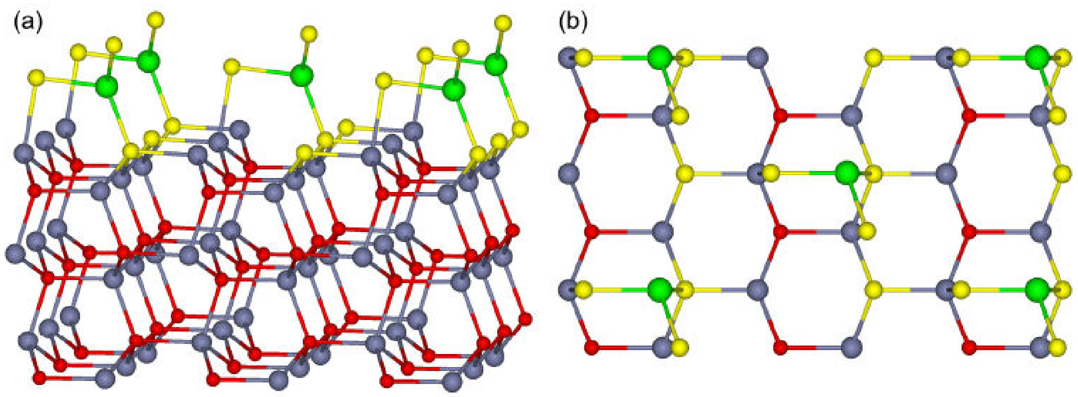

Figure S7. Aside (a) and atop (b) views of 3×3 supercells for S-doped ZnO($1\bar{1}00$)/*s*WS_2 interface with *n*-type morphology of substrate and 0.5ML net configuration of adsorbate. Small red, middle yellow, middle grey-blue and large green balls correspond to O, S. Zn and W atoms, respectively.

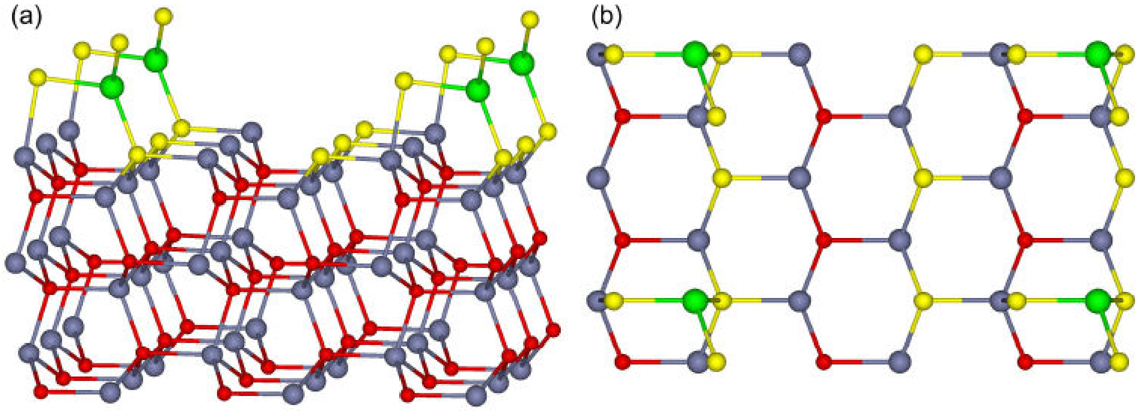

Figure S8. Aside (a) and atop (b) views of 3×3 supercells for S-doped ZnO($1\bar{1}00$)/*s*WS_2 interface with *n*-type morphology of substrate and 0.25ML net configuration of adsorbate. Small red, middle yellow, middle grey-blue and large green balls correspond to O, S. Zn and W atoms, respectively.

Atomistic Models of Monolayer Coverage of Pristine ZnO($1\bar{1}00$) Substrate by WS_2. Figures S9 and S10 show WS_2 monolayer on *n*- and *p*-type ZnO($1\bar{1}00$) substrates, respectively. Because of the difference between the lattice parameters of adsorbate and substrate leading to interfacial strain, 1ML coverage of pristine *n*-type ZnO substrate is found to be energetically less stable than 0.5ML undoped configuration (*cf*. Tables S2 and 2, respectively), due to the difference in coordination. Meanwhile, S-doped ZnO($1\bar{1}00$) slab results in additional strain between the outer and the next O-containing layers, thus additionally reducing E_{bind} (Table 2).

The most essential difference between both interfaces (Table S2) is metallicity of *n*-type *vs.* semi-conductivity of *p*-type accompanied by differences in their structural and energy parameters. Left bottom plot of DOS (Figure S11) and analogous plot for striped configuration of 0.5ML WS_2($1\bar{1}00$) submonolayer show that metallicity is caused by nanothin layer of adsorbate, striped configuration of which hardly can exist.

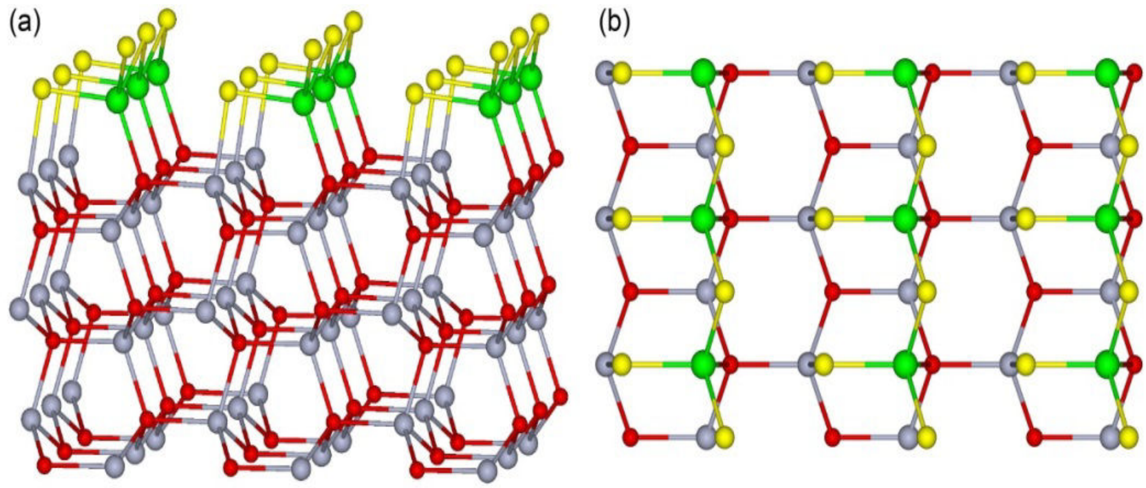

Figure S9. Aside (a) and atop (b) views of 3×3 supercells for ZnO($1\bar{1}00$)/WS_2 interface with *n*-type morphology of substrate and concentration of adsorbate 1ML. Small red, middle yellow, middle grey-blue and large green balls correspond to O, S. Zn and W atoms, respectively.

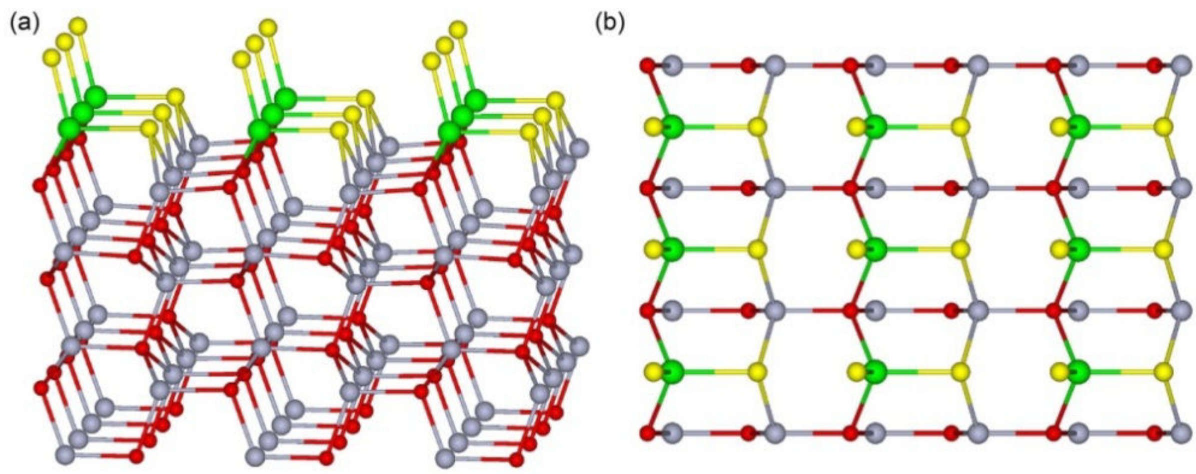

Figure S10. Aside (a) and atop (b) views of 3×3 supercells for ZnO($1\bar{1}00$)/WS_2 interface with *p*-type morphology of substrate with concentrations of adsorbate 1ML. Small red, middle yellow, middle grey-blue and large green balls correspond to O, S. Zn and W atoms, respectively.

Table S2. Energy and geometry parameters of optimized ZnO($1\bar{1}00$)/WS_2 interface models (Figures S9 and S10).

models of interface		E_{bind}, eV	interlayer distances in substrate, Å		interfacial distance, Å	band gap, $\Delta\mathcal{E}_g$, eV
			$h_{inter\text{-}layer\ (outer)}$	$h_{inter\text{-}layer\ (internal)}$		
1ML	*n*-type	1.88	2.82	2.81	2.03	–*
	p-type	2.99	2.76	2.82	1.53	0.24

* conducting states

DOSs for ZnO($1\bar{1}00$) or WS_2(0001) Substrates and ZnO($1\bar{1}00$)/sWS_2 or sWS_2($1\bar{1}00$)/ WS_2(0001) Interfaces. We have performed calculations of one-electron densities of states for both separate constituents of ZnO($1\bar{1}00$)/WS_2 interfaces as well as different morphologies of these interfaces *per se*. Both ZnO($1\bar{1}00$) substrate (Figure S11) and WS_2(0001) adsorbate (Figure S12) are typical semiconductors while WS_2($1\bar{1}00$) monolayer and striped submonolayers manifest semi-metallic properties and conductivity which have not been observed in experiments.

In the case of *s*WS_2($1\bar{1}00$)/WS_2(0001) interfaces and their constituents (Figure S12), we observe semi-conductivity when structural units of adsorbate are separated by distances corresponding to at least second or third coordination spheres (net 0.5ML or net 0.25ML).

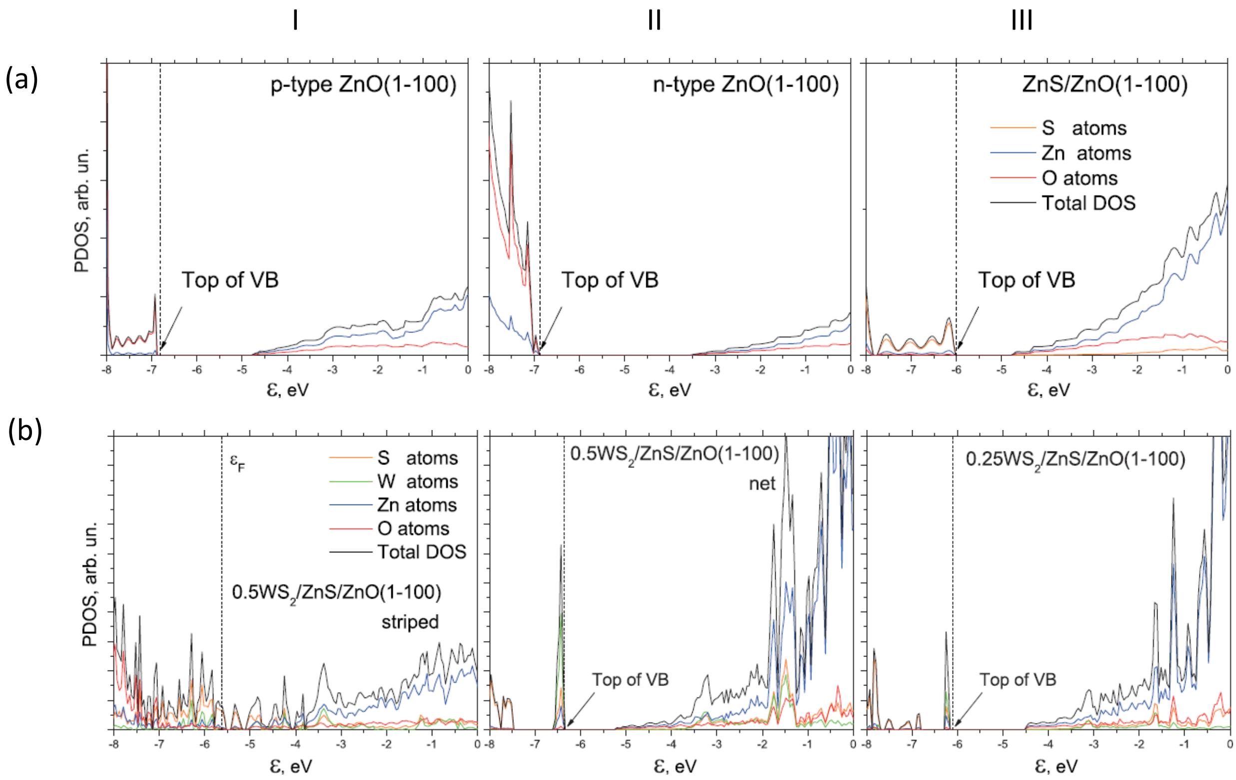

Figure S11. Total and partial densities of states for ZnO($1\bar{1}00$) substrate of *n*- (both pristine and S-doped) and *p*-types (pristine). Top plots: DOSs for ZnO substrate. Bottom plots: DOSs for ZnO($1\bar{1}00$)/sWS_2 interfaces, different configurations of adsorbate are considered: striped 0.5ML, net 0.5ML and net 0.25ML.

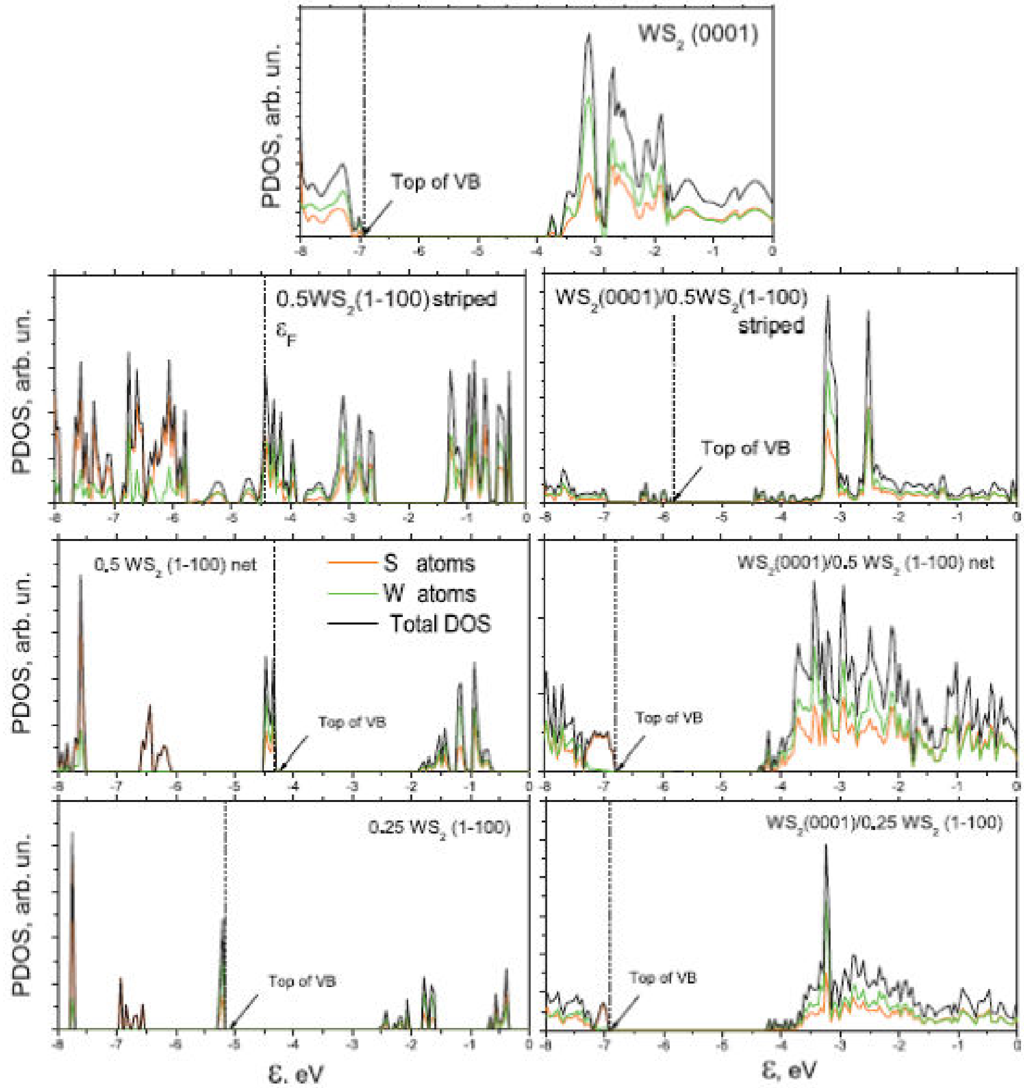

Figure S12. Total and partial densities of states for $WS_2(0001)$ nanolayer (top plot) and for $WS_2(1\bar{1}00)$ submonolayers *per se* (left plots). Right plots describe DOSs for $s$$WS_2(1\bar{1}00)/WS_2(0001)$ interfaces.